A Nonlinear Counts to Antenna Temperature Algorithm for a Total Power Radiometer with External Calibration and Noise Diode Injection

Faisal Alquaied
Electrical and Computer Engineering
University of Central Florida
Orlando, FL, U.S. 32816-2362
falquaied@knights.ucf.edu

W.Linwood Jones
Electrical and Computer Engineering
University of Central Florida
Orlando, FL, U.S. 32816-2362
wlinwoodjones@gmail.com

***Abstract*— The newest innovation to passive microwave remote sensing technology is the inclusion of noise diodes for radiometric calibration of total power radiometers. Instead of the usual two-point calibration using passive black body sources, now there are four-calibration noise levels, which allow system nonlinearities to be corrected. Conventional approaches linearize the radiometer output "rad_counts" (using the four-point calibration correction) and use a linear transfer function to calculate the antenna temperature (T_A) at the radiometer input. This paper presents a novel approach of using a quadratic radiometer transfer function (with nonlinear rad_counts) to derive (T_A). This algorithm is tested using on-orbit satellite measurements from the Global Precipitation Measurement (GPM) Microwave Imager (GMI). Empirical results are presented, which show only mille-Kelvin differences between this T_A algorithm and the standard T_A product provided by NASA.**

I. Introduction

Microwave radiometers are usually designed to be linear systems because it simplifies their system transfer function, between the output (rad_counts) and the input antenna temperature (T_A), to be linearly proportional to the scene radiometric brightness captured by the antenna. However, in a practical sense, all radiometers have nonlinearities, and if significant, the rad_counts are usually corrected for the nonlinearity of the radiometer transfer function. Thus, the calculation of T_A involves the use of linearized rad_counts in a linear system transfer function.

This paper presents an alternate approach, hereafter known as the "CFRSL T_A Algorithm" that uses the nonlinear counts in a quadratic transfer function to calculate the T_A. We assume that the radiometer system non-linearity is characterized in real-time by introducing injected noise to the traditional hot and cold radiometric calibration targets; thereby providing four calibration points to define the system transfer function. The functional block diagram of such a microwave radiometer is shown in Fig. 1, which for illustrative purposes, takes the form of a conically scanning total power radiometer with external black body targets. During each revolution, the main reflector antenna views earth, cold sky, and a hot load black body target. The cold sky calibration point is known at 2.73 K, and the hot load point is a microwave absorber black body with measured physical temperature (typically 300 – 350 K) [1].

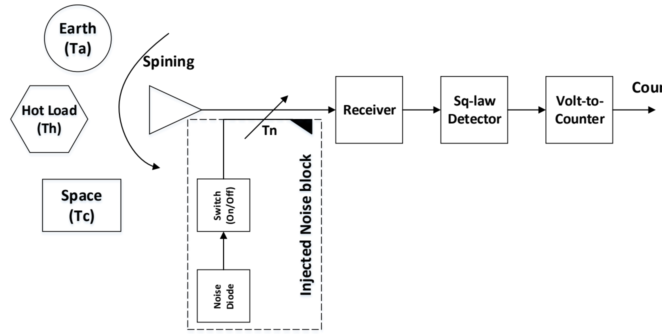

Fig. 1. The block diagram of a radiometer with injected noise and two external calibration black body targets.

In this paper, it is assumed that the nonlinearity of the counts is a quadratic function of the antenna temperature. Since the system has four different calibration points, the counts are expressed as:

$$C_c = S(T_c)^2 + G(T_c) + Offset \quad (1)$$

$$C_h = S(T_h)^2 + G(T_h) + Offset \quad (2)$$

$$C_{cn} = S(T_c + T_n)^2 + G(T_c + T_n) + Offset \quad (3)$$

$$C_{hn} = S(T_h + T_n)^2 + G(T_h + T_n) + Offset \quad (4)$$

where C_c & C_h are the measured counts and T_c, T_h, & T_n are the antenna temperatures of: cold sky, hot load, and noise diode injection, respectively. Also, the C_{cn} and C_{hn} are the measured counts while the noise diode is on. Finally, the unknown parameters are: the quadratic nonlinearity (S), the system gain (G) and the system (dc) offset. Note that the receiver temperature is included in the offset, which is the same for all four equations.

The objective of the calibration process is to determine the four unknown system parameters (*S, G, Offset*, and T_n) by simultaneously solving equations (7) to (10). After determining these unknown parameters and by using the earth scene counts (C_s), the earth scene antenna temperature is:

$$T_{a-cfrsl} = \frac{-G + \sqrt{G^2 - 4S(Offset - C_s)}}{2S} \tag{5}$$

In section II of this paper, the CFRSL antenna temperature algorithm is described and a detailed derivation for each parameter is provided. Section III provides a comparison of this CFRSL algorithm with the standard NASA data processing for the Global Precipitation Measurement (GPM) Microwave Imager (GMI). Results demonstrate that both independent approaches agree very well in the calculated earth scene antenna temperature. Finally, conclusions are presented in Section IV.

II. Algorithm

In this section, the solution of each unknown parameter is provided using (1) to (4). First, the injected noise diode temperature can change over time, therefore it is estimated using the output counts at the four calibration points:

$$T_n = \frac{(T_h - T_c) * (C_c + C_h - C_{cn} - C_{hn})}{(C_c - C_h + C_{cn} - C_{hn})} \tag{6}$$

Likewise, the radiometer non-linearity can change over time, so the parameter *S*, is also estimated using the four calibration points:

$$S = \frac{(C_h + C_{cn} - C_c - C_{hn})}{2T_n * (T_c - T_h)} \tag{7}$$

Similarly, the gain of the system is:

$$G = \frac{S * (T_h^2 - T_c^2) + C_c - C_h}{(T_c - T_h)} \tag{8}$$

Finally, the system dc offset, given in the equations (1) to (4), can be found by using any of these equations since all of the parameters are known. For example, the offset value is expressed by using equation (2):

$$Offset = C_h - S(T_h)^2 - G(T_h) \tag{9}$$

III. Validating/Comparing

This section provides results from a validation experiment using actual satellite microwave radiometer data from the Global Precipitation Measurement (GPM) Microwave Imager (GMI), which was launched on February 27, 2014 [2, 3]. A typical result presented in Fig. 2 is the difference between this CFRSL T_a using (5) and the standard T_A product $T_{a\text{-}gmi}$ defined in [4, 5]. These data are the observed earth scene temperature obtained when the GMI views forward over one orbit. The difference in T_a between the two approaches is presented that ranges between -1 to +10 mille Kelvin. The variance of the

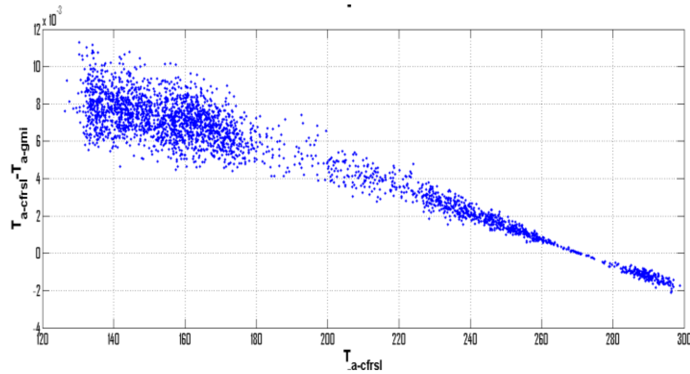

Fig. 2. The difference between Ta-cfrsl and Ta-gmi with earth scene Ta-cfrsl

difference depends upon the earth scene T_a with the minimum occurring ~ 270 K. This appears to be an indication that the nonlinearity is not being totally corrected by one or the other of these T_A algorithms. Moreover, which approach is performs best to remove the nonlinearity has not been determined. Nevertheless, mille-Kelvin differences in the T_a are not a significant effect for most earth remote sensing applications.

IV. Conclusion

This research is a work in progress, and this paper presents a new CFRSL T_A algorithm that uses nonlinear counts and a quadratic radiometer transfer function to calculate the antenna temperature for a radiometer with significant nonlinearity. The algorithm requires 4 radiometric calibration points produced by: cold load, cold load + injected noise, hot load, and hot load+ injected noise. A validation experiment was performed using the GMI as the well-calibrated antenna brightness temperature standard, and preliminary results indicted that the CFRSL algorithm differs < 10 mille-Kelvin over the full dynamic range of on-orbit earth scene antenna temperatures between 150 – 290 K. To date, only a few orbits of data have been analyzed, but the results are encouraging. The most significant negative result, is that there is a systematic Ta difference, which is highly correlated with the earth scene temperature. This suggests that the nonlinearity effect has not been totally eliminated. This is the subject of future investigation.

References

[1] Ulaby, Fawwaz and David Long, “Microwave radar and radiometric remote sensing”, Ann Arbor: University of Michigan Press, 2014, pp. 262-293.

[2] Hou, Y., et al., “The global precipitation measurement mission,” Bull. Amer. Meteorol. Soc., vol. 95, pp. 701–722, 2013.

[3] Draper, David, et al. "The Global Precipitation Measurement (GPM) Microwave Imager (GMI): Instrument Overview and Early On-Orbit Performance," IEEE Journal of Selected Topics in Applied Earth Observations and Remote Sensing, vol. 8, no. 7, pp. 3452-3462, March 2015.

[4] Draper, David W., et al. "Assessing Calibration Stability Using the Global Precipitation Measurement (GPM) Microwave Imager (GMI) Noise Diodes," IEEE Journal of Selected Topics in Applied Earth Observations and Remote Sensing, vol. PP, no. 99, pp. 1-9, March 2015.

[5] T. Meissner and F. J. Wentz, “GMI calibration algorithm and analysis theoretical basis document,” Remote Sens. Syst., Santa Rosa, CA, USA, Rep. 051707, 2012.